Reversible Surface Wettability by Silanization

Marius Brehm, Johannes M. Scheiger, Alexander Welle, and Pavel A. Levkin*

The chemistry and wettability of oxygen containing surfaces can be conveniently modified by silanization with various organosilanes which form Si—O bonds on the surface. This work shows that a superhydrophobic nanoporous polymer coating can be reverted to its previous hydrophilic state by removing the fluoroalkyl silane with fluoride anions using tetrabutyl ammonium fluoride. This leads to a completely reversible process of silanization and desilanization which can be performed in less than 2 min for each step as proven by droplet shape analysis and secondary ion mass spectrometry. Additionally, the desilanization solution can be applied spatially by an automated liquid dispenser or manually by a brush, leading to patterns with different wettability, such as droplet microarrays or liquid channels.

1. Introduction

Over recent decades, controlling surface wettability has received a great deal of attention[1] due to its potential applications in processes such as oil-water separation,[2] self-cleaning surfaces,[3] corrosion inhibition,[4] or anti-biofouling.[5] Spatial control of surface wettability also allows for discontinuous dewetting and microfluidic applications.[6]

M. Brehm, J. M. Scheiger, Dr. P. A. Levkin
Karlsruhe Institute of Technology (KIT)
Institute of Toxicology and Genetics (ITG)
Hermann-von Helmholtz-Platz 1, Eggenstein-Leopoldshafen
76344, Germany
E-mail: levkin@kit.edu
Dr. A. Welle
Karlsruhe Institute of Technology (KIT)
Institute of Functional Interfaces
Hermann-von Helmholtz-Platz 1, Eggenstein-Leopoldshafen
76344, Germany
Dr. A. Welle
Karlsruhe Institute of Technology (KIT)
Karlsruhe Nano Micro Facility
Hermann-von Helmholtz-Platz 1, Eggenstein-Leopoldshafen
76344, Germany
Dr. P. A. Levkin
Karlsruhe Institute of Technology (KIT)
Institute of Organic Chemistry
Karlsruhe 76131, Germany

The ORCID identification number(s) for the author(s) of this article can be found under https://doi.org/10.1002/admi.201902134.

The key to achieving superhydrophobicity (SH) is a suitable combination of surface structure and chemistry.[7] Based on the physical descriptions by Young, Wenzel, Cassie, and Baxter, surface roughness and low surface energy are crucial properties for this purpose and need to be controlled.[8–10] As the best known example of superhydrophobicity in nature, the surface of the lotus leaf is covered with microscaled pillars overlaid with a hydrophobic wax.[11] While alkylated or fluorinated materials are the most common chemical constituents of artificial superhydrophobic surfaces, diverse, and sophisticated methods of surface structuring have been developed including lithography,[12] laser structuring,[13] polymer phase separation,[7] silicon nanograss,[14] and carbon nanotubes.[15] Furthermore, strategies to induce the transition of a surface between the hydrophilic and hydrophobic states have been developed and extensively studied.[16] For example, the wetting behavior of oxides of tin,[17] zinc,[18] and tungsten[19] are altered by UV irradiation due to a photoinduced radical rearrangement process. While the metal oxides are superhydrophobic after manufacturing, they rapidly become hydrophilic after irradiation. However, this transition is temporary and the metals slowly return to the thermodynamically more stable superhydrophobic state when placed in darkness. Another method that achieves a more stable transition is UV-triggered azobenzene isomerization, which is based on the change in polarity induced by a cis/trans transition of surface-bound azobenzene compounds.[20] Although the transition is rapid and easily reversible by irradiation with different wavelengths, the surface will not reach a superhydrophilic state due to the non-polar aromatic systems.[21] Similar drawbacks are encountered when the surface topology is modified via an external electric field.[22]

To achieve complete conversion between the superhydrophilic and superhydrophobic states on the same structured surface it requires significant changes in the chemistry of the surface, which must remain stimuli-responsive for reversibility. Our recently published UV-triggered disulfide exchange reaction on a surface complies with these specifications.[23] The disulfide bond formed is not only more stable than the bonds formed by imines,[24] but also allows for a versatile reversible patterning as a result of the spatially controlled and rapid interchange of surface chemistry. However, one can conceive of a surface that demands stable, yet switchable wettability without the possibility for UV irradiation. Attempts based on host-guest interaction[25] or counterion exchange[26] may also allow for a fast switch in surface wettability, but lack the high stability of covalently bound modifiers like the very stable Si—O bond of a silanized surface.

**ADVANCED
SCIENCE NEWS** _____
www.advancedsciencenews.com

**ADVANCED
MATERIALS
INTERFACES**
www.advmatinterfaces.de

Thus, we propose the concept of the reversible modification of polymer or silicon surfaces by silanization and desilanization. While the silanization process is not new and is somewhat standard in surface chemistry, it is regarded as permanent (except for unselective laser ablation[27]), although the specific cleavage of the silicon–oxygen bond by fluoride ions is also a well-established method in organic chemistry.[28]

In this study, we investigated the influence of the simple and rapid process of silanization and desilanization on wettability of a nanorough polymer coating or silicon wafer. We demonstrated that the transition from the hydrophilic to the superhydrophobic state in case of the structured polymer and vice versa can be accomplished in 2 min or less and can also be spatially controlled by automated liquid dispensing or manual "drawing".

2. Results and Discussion

2.1. Water Contact Angles

The surface wettability was determined by measuring the static, advancing, receding, and sliding contact angles of water droplets. The values for the unmodified hydrophilic and the silanized superhydrophobic polymer surfaces are shown in **Table 1**.

Because of the porosity of the polymer and its hydrophilicity, we were not able to obtain reliable measurements of the advancing and receding WCA. Nevertheless, the very low static contact angle of 6° confirms the highly hydrophilic state of the surface and as expected, a sliding angle was also not observed. Is should be noted that this value does not represent the classic water–solid contact angle, but is the contact angle between the water droplet and the liquid-infused surface of the porous polymer. This effect is visible in **Figure 1**, where some of the water first enters the pores by capillary action followed by gradual formation of a droplet on the wetted surface.

Treatment of the polymer-coated surface with the silanization solution containing 2% (v/v) TCPS in toluene for 2 min greatly increased the water contact angles and established a superhydrophobic state on the surface with a static WCA of 160° and a sliding angle of less than 10° (see detailed data in Table 1).

2.2. Silanization Process

The kinetics of the silanization reaction were determined by measuring the WCA at different time-points after immersion of

Table 1. The water contact angles (WCA) of the unmodified (hydrophilic) and TCPS-modified (superhydrophobic) polymer surfaces. Data were obtained by measuring with a 10 µL water droplet. Data represent the mean of five measurements at different locations on the surface; standard deviation is shown in parentheses.

	Hydrophilic	Superhydrophobic
Static WCA	6° (±1)	160° (±1)
Advancing WCA	–	162° (±1)
Receding WCA	–	153° (±3)
Sliding WCA	–	9° (±4)

a polymer-coated slide in the silanization solution (**Figure 2A**). Although the static WCA reached a maximum after 30 s of immersion, the sliding WCA reached a minimum only after 2 min of immersion. We calculated the contact angle hysteresis as the difference between advancing and receding WCAs, and its decline was dominated by the changing kinetics of the receding WCA, since the advancing WCA reached the endpoint after the first 15 s, while the receding WCA changed at a slower rate (45 s). These measurements demonstrate that the silane modification of the polymer coating is complete after 2 min of immersion in a solution of 2% (v/v) TCPS in toluene at room temperature.

We further analyzed the silanized polymer surface via ToF-SIMS to gain a more detailed view of the chemistry (**Figure 3**). An X-Y-scan of the surface after the modification and the following plot of measured ion concentration received from TCPS-correlated fragments [Si^+ (Figure 2C) and CF_3^+ (Figure 2D)] confirmed the presence of the silane modification all over the polymer surface as a coherent and uniform layer. Thus, we have demonstrated that it is possible to achieve rapid surface modification (silanization) by simple immersion in the solution without the need for initiators or heating.

2.3. Desilanization Process

Surface modification via silanization is based on the formation of a silyl ether; therefore, the free hydroxy groups can be restored by cleaving this silicon–oxygen bond to change the surface chemistry and wettability. Traditionally in organic synthesis, this is performed by the addition of fluoride anions in the form of TBAF, HF, or NaF.[29] The driving force of this reaction as presented in **Scheme 1** is the formation of the very stable Si—F bond whose bond energy is around 172 kJ mol^{-1} higher than the energy of the Si–O bond (369 and 541 kJ mol^{-1}).[30]

To investigate the speed of this process, we measured the changes in WCA of a previously silanized polymer-coated slide immersed in two concentrations of TBAF for different time periods. As shown in Figure 2B, the kinetics of the silyl ether cleavage is dependent on the concentration of fluoride ions added via TBAF, but is generally rapid. Total surface wettability was achieved after just 10 s of immersion in 1 M TBAF and prolonged immersion had no further effect on the static WCA. Following immersion of the modified surface in a solution containing 0.1 M TBAF, a transition to decreased wettability was observed which delayed the endpoint of the reaction to 60 s of immersion. Again, prolonged immersion in the TBAF solution has no further effect on wettability. The intermediate contact angle measurements showed a continuous decrease in the static WCA during the immersion as the amount of free hydroxyl groups increased. A TCPS silanized polymer-coated slide was immersed in pure THF for the same amount of time, but showed no significant change in wettability (Figure 2B). This indicates a stable modification of the surface.

2.4. Reversible Wettability

To show the total reversible wettability, cylces of silanization and desilanization was performed and the static WCA was
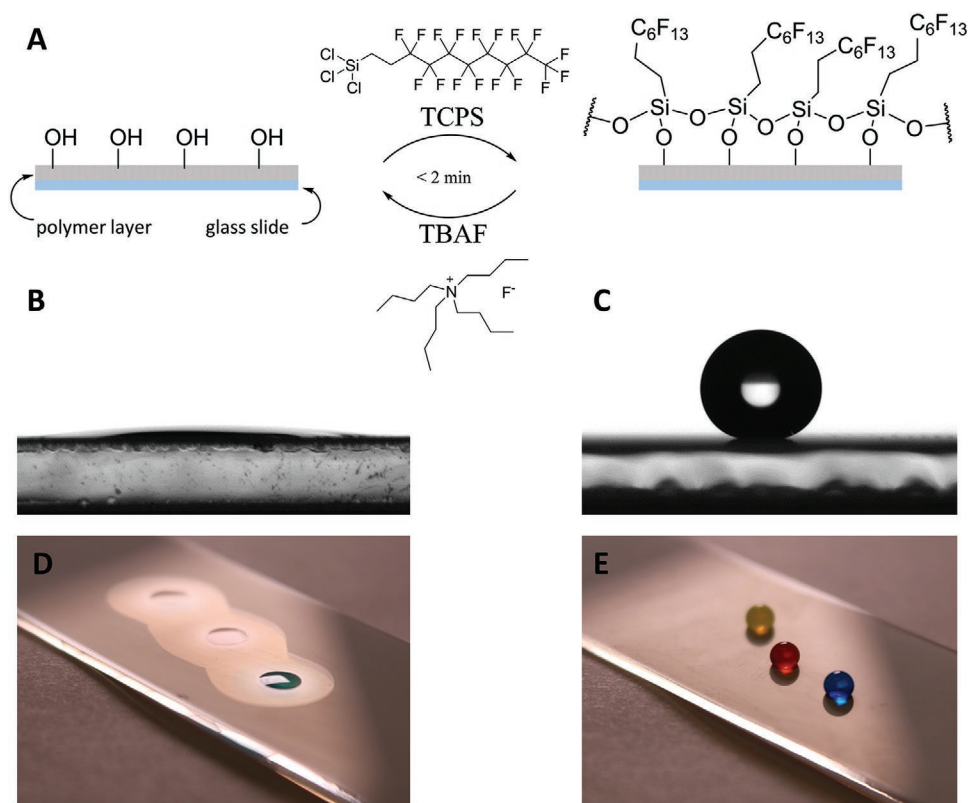
Figure 1. General overview of the method as a reaction scheme (A) and images of water droplets on hydrophilic (B,D) and superhydrophobic (C,E) polymer surfaces. A) The nanoporous HEMA-co-EDMA polymer on a glass support is hydrophilic due to its hydroxyl groups and can be rapidly modified to exhibit superhydrophobicity with 1H,1H,2H,2H-trichloroperfluorooctylsilane (TCPS). This process is completely reversible by treatment with tetra-*n*-butylammonium fluoride (TBAF). Each step can be performed in 2 min. (B,C) Screen captures of water droplets from the water contact angle analysis. (D,E) Photographs of pipetted aqueous food dye solutions.

measured after very step. Figure 2B shows the progressive changes in the static WCA after each step, starting with a non-modified nanoporous HEMA-co-EDMA copolymer in step 1. The immersion time for every silanization and desilanization step was 2 min and the TBAF concentration was 0.1 M. The average static WCA for the hydrophilic states was measured as 7° with a standard deviation of 1°. In the hydrophobic states, the surface showed an average static WCA of 159° with a standard deviation of 3°. These results demonstrate that the WCA achieved remained stable over 16 steps representing eight full cycles. Summarized after this experiment, the polymer substrate had been immersed in the TBAF solution for 30 min (15 × 2 min) and was still mechanically stable against blow drying with an air gun. Further stability studies via AFM are presented in the Supporting Information.

To confirm the total chemical reversibility of our process, we analyzed the turnover of this cycle via ToF-SIMS. Three samples were prepared: a freshly produced non-modified polymer-coated slide (Figure 3B), a TCPS-modified polymer-coated slide (Figure 3C) and a desilanized sample of the latter (Figure 3D).
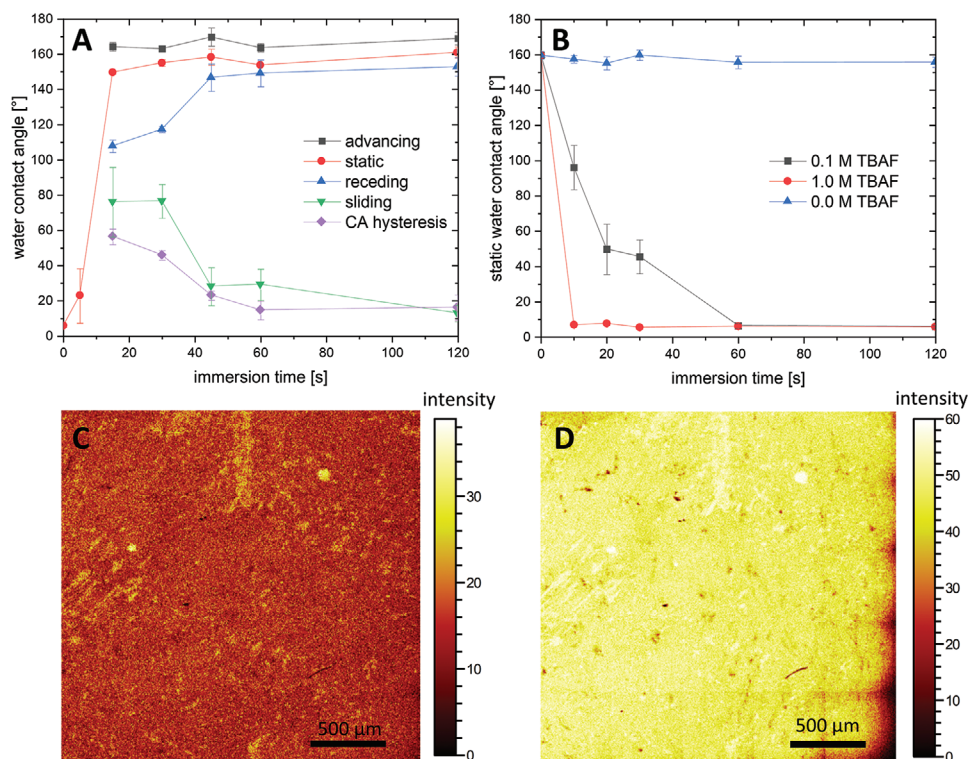
By argon cluster bombardment during the ToF-SIMS measurement, the entire polymer layers of all three samples were eroded and sampled. The ion intensity of CF^+ at 30.997 m/z and a signal corresponding to the polymer (CH_3O^+) at 31.017 m/z were summed as a reference. As expected, there was no ion signal corresponding to the TCPS modification at the start of the cycle prior

to exposure to the silanization solution. After the modification was completed and the polymer coating was converted to the superhydrophobic state, the emergence of CF^+ signal (and others) indicated the presence of the fluoroalkylsilane. Following desilanization of the sample, the peak correlating to the modification was lost, thus demonstrating the total reversibility of the modification of the functional groups on the surface.

2.5. Applicability of Other Silanes and Silicon Surfaces

To test the versatility of our method, we modified samples of the polymer coating with trichlorododecylsilane and trimethylchlorosilane. Both silanes changed the prior hydrophilic polymer (static WCA 6° ± 1) to hydrophobic surfaces with static water contact angles of 110° (±2) for trichlorododecylsilane and 102° (±1) for trimethylchlorosilane (see **Figure 4**A,B). By immersion in the TBAF solution for 2 min, the WCAs decrease again to 7° (±2) for both surfaces, indicating the removal of the silanes.

Additionally, we tested the reversibility on silicon wafers as substrate (Figure 4C). Plain Si wafers show a water contact angle of 30° (±1), which increases to 107° (±3) after the modification with TCPS. In contrast to the polymer film, treatment under standard conditions with TBAF for 2 min does not completely restore the initial surface, which is observed by a contact angle of 55° (±1). However, after a prolonged treatment of 24 h,

**ADVANCED
SCIENCE NEWS**

www.advancedsciencenews.com

**ADVANCED
MATERIALS
INTERFACES**

www.advmatinterfaces.de

Figure 2. Water contact angles for the monitored silanization and desilanization processes and ToF-SIMS mapping of the modified surface. A) The kinetics of surface superhydrophobicity development by immersion in the silanization solution (2% (v/v) TCPS in toluene). The hydrophobicity end-point is reached after the first 15 s, while the superhydrophobic endpoint is reached after 2 min. Each data point represents the average value of three measurements at different positions on the surface. Error bars represent the standard deviation. B) The kinetics of desilanization depend on TBAF concentration. Silanized slides were treated with different concentrations of TBAF in the desilanization solution. Lowering the concentration resulted in a slower conversion. Each data point represents the average value of three measurements at different positions on the surface. Error bars represent the standard deviation. C,D) ToF-SIMS analysis of the TCPS silanized surface shows the presence of fluorinated alkylsilanes indicated by the detection of Si^+ (C) and CF_3^+ (D) ion signals.

the water contact angle further decreased to 35° (±3), indicating reversibility for silicon substrates under longer reaction times.

2.6. Generation of Droplet Microarrays by Liquid Dispensing
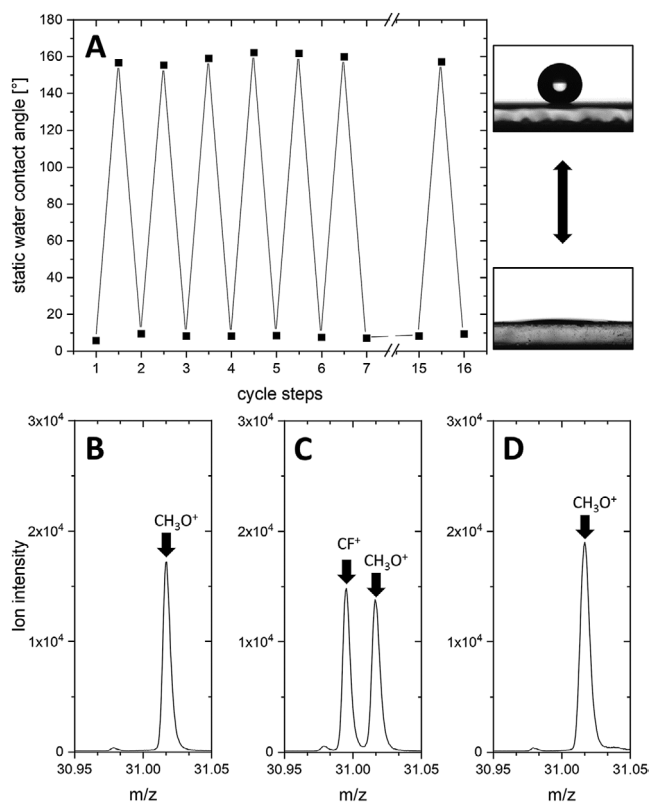
To evaluate the potential for an additional application of this method, we performed the reversible modification spatially on the surface. Using an automatic contactless liquid dispensing system (iDOT), we applied the reaction solution to distinct points on the surface. Starting with a TCPS-modified superhydrophobic nanorough polymer surface and applying the desilanization solution in a spatial configuration, we generated an array of wettable spots surrounded by a superhydrophobic background. However, due to the rapid evaporation of common non-polar organic solvents like THF, which was used for the desilanization process, we needed to select a more suitable solvent system for this application. The main requirement was a low vapor pressure, so that even small volumes (in the nano-liter range) would be non-volatile and remain on the surface long enough to allow the reaction to occur. On the other hand, highly polar solvents with a high surface tension (e.g., water) would neither wet the superhydrophobic surface, nor react with it. With that in mind, we selected 10% (v/v) of THF in GBL as a solvent and a TBAF concentration of 0.1 м.

The non-contact liquid dispensing system (iDOT) was programmed to print 8 nL of the TBAF solution in an array of spots with a spot-to-spot distance of 1.5 mm. After dispensing and 2 min of reaction time, the slide was briefly immersed in ethanol to wash off the TBAF. After drying the polymer with an air gun, the surface was rinsed with deionized water and a discontinuous dewetting occurred, yielding a self-forming array of distinct droplets due to the wettability contrast of the super-hydrophobic background and the hydrophilic spots.

The analysis of this surface via ToF-SIMS is shown in **Figure 5**A–C. The pictures show a 3 x 3 mm sector containing four spots with a diameter of 1 mm. We focused our analysis on the spatial quantification of the CF^+ (Figure 5A), H^+ (Figure 5B), and $C_2F_3^+$ (Figure 5C) ions to follow the desilanization reaction on the polymer layer. All ion signals showed distinct round spots with a diameter of 1 mm and differing chemistry compared to the surrounding background. The edges of the spots were clearly defined since the reaction occurs only in the areas wetted with the desilanization solution.

The signals at 68.99 m/z and 80.98 m/z, which represent fragments of the fluorinated silanes CF^+ and $C_2F_3^+$, were significantly decreased in the hydrophilic areas indicating the chemical conversion of fluorinated silyl ether to free hydroxyl groups by the cleavage of the silyl ether. Additionally, as the chemical environment in the spots changed, the ionization tendency of

**ADVANCED
SCIENCE NEWS**

www.advancedsciencenews.com

**ADVANCED
MATERIALS
INTERFACES**

www.advmatinterfaces.de

Figure 3. Static water contact angles for reversible surface modification cycles and ToF-SIMS analysis of one cycle. A) Silanization and desilanization processes were alternated and the static water contact angles were measured after every conversion. The WCA achieved remained stable even after 16 steps. Lower panels: Depth integrated SIMS data of polymer layers: B) non-treated, C) TCPS-silanized, and D) desilanized. The polymer was thoroughly eroded during measurement and the intensity of the CF^+ and CH_3O^+ ions were summarized for the whole layer. No excess CF^+ was detected after the TBAF treatment, indicating complete conversion.

hydrogen ions was also altered (Figure 5B), which was detectable as a lower ion intensity for H^+ in the spots.

To better visualize of the distinct wettable spots, we added 500 nL of food dyes dissolved in deionized water to every spot. A close-up image of the droplets forming a microarray of free standing droplets on the polymer surface is shown in Figure 5D,E.

2.7. Hydrophilic Channels Drawn Manually by Brush Writing

Greater flexibility in the design and creation of hydrophilic areas on the hydrophobic background can be achieved by using
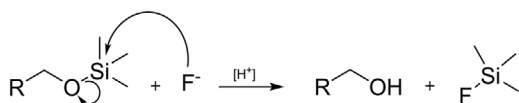
Scheme 1. Mechanism of trimethylsilyl ether cleavage by fluoride anions, followed by protonation of the alkoxide.[28] Driving force is the high Si—F bond energy.

an artist's brush to spread the desilanization solution on the polymer coating. A solution of 0.1 M TBAF in 10% (v/v) THF in GBL was prepared for use in the same way as an ink or dye (see **Figure 6**A). The brush was dipped into this solution and used to draw a channel on a TCPS-modified surface as shown in Figure 6B. After a reaction time of 2 min, the solution was washed off with ethanol and the surface was dried under an air flow. Once dry, no pattern was visible on the polymer coating; however, by applying a stream of water on the slightly tilted slide, the different wettability conditions caused a channel to form spontaneously as the water flowed off the surface. The hydrophobic background stabilized the stream even at higher flow rates. A video of the preparation process and channel formation is shown in Supporting Information. The method is not just limited to simple channels, and various shapes can be drawn (Figure 6C,D) showing the simplicity and versatility of our method.

3. Conclusion

The rapid and versatile modification of suitable materials via silanization to change their chemical and physical properties is a basic procedure in surface science. Furthermore, the conversion of a hydroxy group to a silyl ether —for example via trimethyl silyl chloride (TMS-Cl)—is a well-known method used by synthetic chemists to protect free hydroxyl groups during multi-step synthesis. For the latter methods, the fast and selective cleavage of the Si—O bond via fluoride anions is important and makes this strategy so convenient. In this study, we combined synthetic and surface chemistry to achieve variable control of surface wettability by either coupling a fluorinated alkyl silane (TCPS) to the naturally hydrophilic surface of a HEMA-co-EDMA nanoporous polymer coating to achieve superhydrophobicity or by removing it from the surface by application of fluoride anions to regain hydrophilicity. The changes in WCA and ToF-SIMS analysis showed that this process is completely reversible in either direction in 2 min. Moreover, the spatial application of fluoride anions in a TBAF solution allowed us to form various and flexible patterns. For greater flexibility, the solution can also be applied manually using an artist's brush. Using this method, hydrophilic channels were formed allowing rapid flow of the water over the surface following the manually drawn hydrophilic path on a superhydrophobic surface. In conclusion, we have achieved rapid, reversible, and versatile control of surface wettability by modification of hydrophilic surfaces with fluorinated alkyl silane and its spatial cleavage by fluoride anions.

4. Experimental Section

Materials and Methods: Toluene, tetrahydrofuran (THF), ethanol, acetone, 1-decanol, gamma-butyrolactone (GBL), 37% (w/w) hydrochloric acid, and ethylene glycol dimethacrylate (EDMA) were purchased from Merck (Darmstadt, Germany). 1H,1H,2H,2H-Trichloroperfluorooctylsilane (TCPS) and 3-(methacryloyloxy) propyltrimethoxysilane were purchased from Alfa Aesar (Karlsruhe, Germany). Tetrabutyl ammonium fluoride trihydrate (TBAF), trichlordodecylsilane, chlortrimethylsilane, sodium hydroxide (NaOH), cyclohexanol, 2,2-dimethoxy-2-phenylacetophenone (DMPAP), and
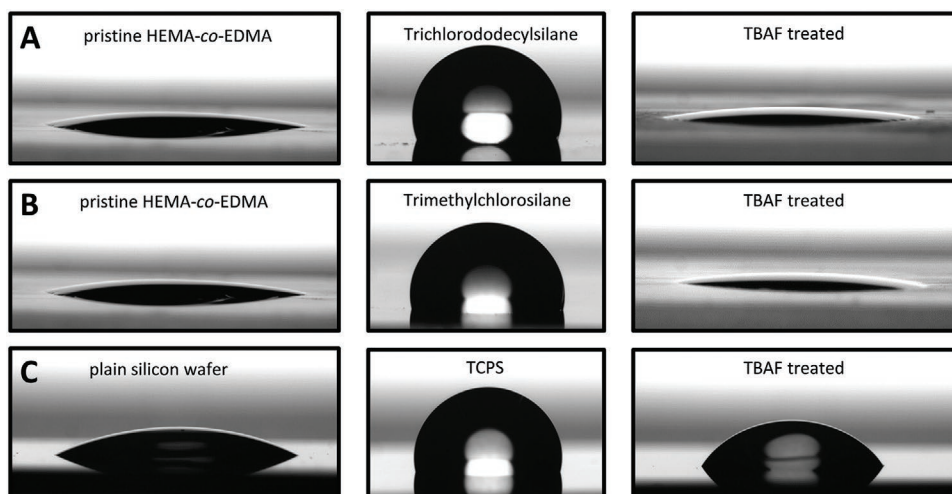
Figure 4. Developed water contact angles of each 10 µL deionized water on pristine, silanized, and desilanized HEMA-co-EDMA (A,B) and silicon surfaces (C). First column shows the plain surfaces with static WCA of 6° (A,B) and 30° (C). Modification of the respective surfaces with either Trichlorododecylsilane, Trimethylchlorosilane or TCPS yielded contact angles of 110°, 102°, and 107°. Treatment with the TBAF desilanization solution for 2 min changes the contact angles to 7° for the polymer surface and 55° for the silicon wafer. Prolonged treatment of the wafer for 24 h in the desilanization solution further decreases the static WCA to 35°.

2-hydroxyethyl methacrylate (HEMA) were purchased from Sigma-Aldrich (Darmstadt, Germany). Microscopy glass slides (76 × 26 mm) were purchased from Schott (Mainz, Germany). All chemicals were used without further purification. Silicon wafers were purchased from Siegert Wafer (Aachen, Germany) with the following specifications: 4P0/5-10/525 ± 20/SSP/TTV<5.

HEMA-co-EDMA Polymer Coating of Glass Slides: A microscopy glass slide was activated by sequential immersion in 1 M aqueous NaOH and 1 M aqueous HCl (1 h each).[31] The hydroxyl groups formed on the surface were then modified by applying a 20% (v/v) solution of 3-(trimethoxysilyl)propyl methacrylate in ethanol for 30 min twice. After

washing with ethanol and drying under air flow, 30 µL polymerization mixture [24% (w/v) 2-hydroxyethyl methacrylate (HEMA), 16% (w/v) ethylene glycol dimethacrylate (EDMA), 25% (w/v) 1-decanol, 34.6% (w/v) cyclohexanol and 0.4% (w/v) 2,2-dimethoxy-2-phenylacetophenone (DMPAP)] was spread on the surface of the slide, which was then placed face down on a fluorinated glass slide. Fluorination of glass slides was carried out by treating an activated slide with 1H,1H,2H,2H-Trichloroperfluorooctylsilane in the gas phase for 16 h and subsequent washing with acetone. The coating was polymerized by UV irradiation at 254 nm (4 mW cm^{-2}, BioLink 254, Vilber Lourmat, Eberhardzell, Germany) for 15 min.
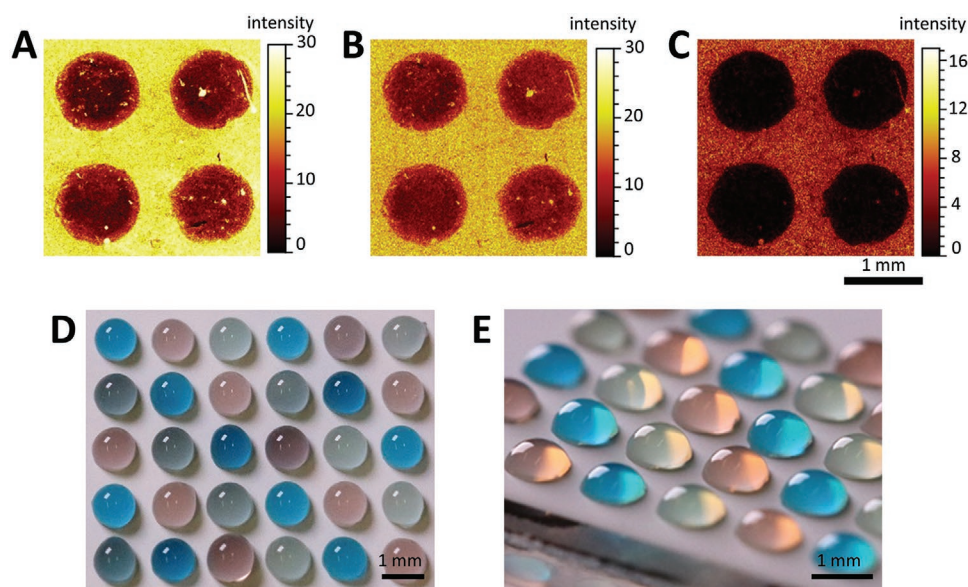
Figure 5. 2D mapping of ToF-SIMS analysis of a spatially desilanized surface (A–C) and photographs of aqueous food dyes in this microarray (D,E). The TCPS-modified surface was printed with 8 nL of 0.1 M TBAF in 10% (v/v) THF in GBL by the automatic liquid dispensing system (iDot); the reaction time was 2 min. Top panels show the lateral distribution of the signal intensity of the CF$^+$ (A), H$^+$ (B) and C$_2$F$_3^+$ (C) ions where the difference in surface chemistry is visible. (D,E) Image of the droplet microarray with a spot diameter of 1 mm and a spot-to-spot distance of 1.5 mm (500 nL of aqueous solutions of food dyes per spot were used for better visualization).
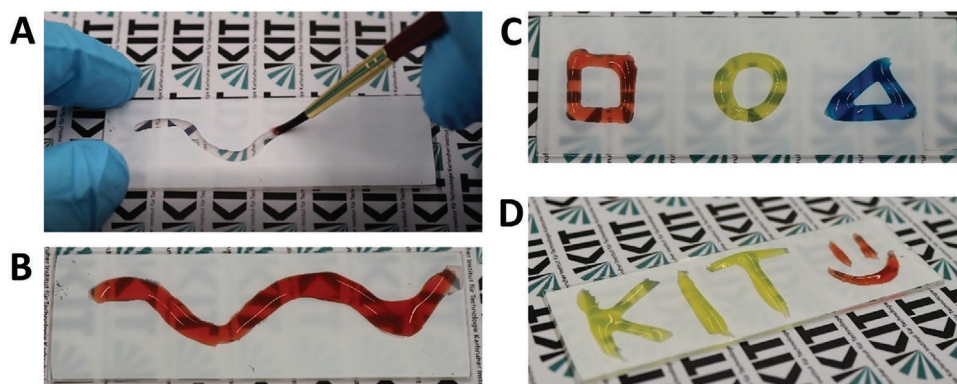
Figure 6. Photographs of the brush writing method (A) and the resulting patterns (C–D). The desilanization solution can be applied using a brush dipped into the liquid. A) Image shows the simple process of designing a fluid channel on a hydrophobic background. B) After a 2-min reaction, the liquid is washed off and the channel is filled with aqueous food dye for better visualization. A video of how this channel is formed and stabilizes flowing water is shown in Supporting Information. (C) and (D). Images show examples of hand-made hydrophilic patterns in which aqueous dye solutions are held.

Surface Modification via Silanization: A polymer-coated glass slide or silicon wafer was immersed in 2% (v/v) TCPS solution in dry toluene for 2 min and washed extensively with acetone and ethanol before drying with an air gun. For the kinetic investigation, the immersion time was varied. Trichlordodecylsilane and chlortrimethylsilane were used accordingly.

Surface Desilanization by Immersion: To regain the unmodified polymer or silicon surface, the silane-modified surface was immersed in a solution of TBAF in THF for 2 min, washed with ethanol and dried with an air gun. For the kinetic investigations, the concentration, and immersion time were varied. As a fluoride containing compound, TBAF must not be acidified due to the formation of highly toxic gaseous hydrogen fluoride. Dissolved in THF, peroxide formation is possible during storage.

Water Contact Angle Measurements: For determination of water contact angles (WCA), the droplet shape of 10 µL of deionized water was analyzed using a DSA25 drop shape analyzer by Krüss (Hamburg, Germany) and the manufacturer's software. The static WCA was determined for a droplet at equilibrium after placement on the surface. Advancing and receding angles were measured by slowly (0.1 µL s^{-1}) adding and removing water from the droplet at the same speed. Sliding angles were determined for a free-standing droplet placed on a table tilted at a speed of 1° s^{-1}.

Wettability Cycles: For reversible modification of the polymer surface, silanization (2% (v/v) TCPS in dry toluene) and desilanization (0.1 M TBAF in THF) via immersion were performed with a measurement of the static WCA between each step. The surfaces were washed extensively with acetone and ethanol and carefully dried to avoid contamination of the solutions or disturbance of the measurements.

Superhydrophobic–Hydrophilic Pattern printed by Liquid Dispenser: The iDot by Dispendix (Stuttgart, Germany) was used for contactless liquid dispensing. The array of spots was generated with a center-to-center distance of 1.5 mm using the programmed printing pattern in the manufacturer's software. Subsequently, 8 nL of a 0.1 M solution of TBAF in 10% (v/v) THF in GBL was printed onto each spot. The reaction was incubated at room temperature for 2 min before immersion in ethanol to wash off the reaction liquid.

Time-of-Flight Secondary Ion Mass Spectrometry: ToF-SIMS was performed on a TOF.SIMS5 instrument (IONTOF GmbH, Münster, Germany). This spectrometer is equipped with a Bi cluster primary ion source and a reflectron type time-of-flight analyzer. UHV base pressure was below 5×10^{-8} mbar. For high mass resolution, the Bi source was operated in a bunched mode providing short Bi^{3+} primary ion pulses at 25 keV energy, a lateral resolution of ≈4 µm, a target current of 0.35 pA. The short pulse length of 0.95 ns allowed for high mass resolution. For large fields of view, both, the sample stage and the primary ion beam were rastered. For static SIMS images primary ion doses were kept below 10^{11} ions cm^{-2}. For charge compensation an electron flood gun providing electrons of 21 eV was applied and the secondary ion reflectron tuned accordingly. Spectra were calibrated on the omnipresent C$^-$, C$_2^-$, C$_3^-$, or on the C$^+$, CH$^+$, CH$_2^+$, and CH$_3^+$ peaks. Based on these datasets the chemical assignments for characteristic fragments were determined. As the thickness of the polymer layer exceeds the probing depth of static SIMS (a few nm) depth integrated spectra were obtained with full erosion of the polymer layer by an argon cluster ion beam, 20 keV, Ar$_{1300}$. This erosion beam was rastered across 800×800 µm and with a non-interlaced timing scheme data were recorded from a concentric 500×500 µm field of view.

Atomic force microscopy: Atomic force microscopy measurements were conducted on a Dimension Icon AFM from Bruker (Billerica, USA) using micro cantilevers from Olympus (Tokio, Japan) with a resonance frequency of ca. 300 kHz.

Data analysis was done with Nanoscope Analysis from Bruker (Billerica, USA).

Supporting Information

Supporting Information is available from the Wiley Online Library or from the author.

Acknowledgements

Conflict of Interest

The authors declare no conflict of interest.

Keywords

[1] L. Feng, S. Li, Y. Li, H. Li, L. Zhang, J. Zhai, Y. Song, B. Liu, L. Jiang, D. Zhu, *Adv. Mater.* **2002**, *14*, 1857.

[2] J. Yong, J. Huo, F. Chen, Q. Yang, X. Hou, *Phys. Chem. Chem. Phys.* **2018**, *20*, 25140.

[3] R. Blossey, *Nat. Mater.* **2003**, *2*, 301.

[4] E. Vazirinasab, R. Jafari, G. Momen, *Surf. Coat. Technol.* **2018**, *341*, 40.

[5] I. Banerjee, R. C. Pangule, R. S. Kane, *Adv. Mater.* **2011**, *23*, 690.

[6] E. Ueda, P. A. Levkin, *Adv. Mater.* **2013**, *25*, 1234.

[7] P. A. Levkin, F. Svec, J. M. J. Fréchet, *Adv. Funct. Mater.* **2009**, *19*, 1993.

[8] T. Young, *Philos. Trans. R. Soc. London* **1805**, *95*, 65.

[9] R. N. Wenzel, *Ind. Eng. Chem.* **1936**, *28*, 988.

[10] A. B. D. Cassie, S. Baxter, *Trans. Faraday Soc.* **1944**, *40*, 546.

[11] W. Barthlott, C. Neinhuis, *Planta* **1997**, *202*, 1.

[12] D. Öner, T. J. McCarthy, *Langmuir* **2000**, *16*, 7777.

[13] T. Baldacchini, J. E. Carey, M. Zhou, E. Mazur, *Langmuir* **2006**, *22*, 4917.

[14] C. Dorrer, J. Rühe, *Adv. Mater.* **2008**, *20*, 159.

[15] H. Li, X. Wang, Y. Song, Y. Liu, Q. Li, L. Jiang, D. Zhu, *Angew. Chem., Int. Ed.* **2001**, *40*, 1743.

[16] S. Wang, Y. Song, L. Jiang, *J. Photochem. Photobiol., C* **2007**, *8*, 18.

[17] W. Zhu, X. Feng, L. Feng, L. Jiang, *Chem. Commun.* **2006**, *26*, 2753.

[18] H. Liu, L. Feng, J. Zhai, L. Jiang, D. Zhu, *Langmuir* **2004**, *20*, 5659.

[19] S. Wang, X. Feng, J. Yao, L. Jiang, *Angew. Chem., Int. Ed.* **2006**, *45*, 1264.

[20] L. M. Siewierski, W. J. Brittain, S. Petrash, M. D. Foster, *Langmuir* **1996**, *12*, 5838.

[21] W. Jiang, G. Wang, Y. He, X. Wang, Y. An, Y. Song, L. Jiang, *Chem. Commun.* **2005**, 3550.

[22] O. Guselnikova, J. Svanda, P. Postnikov, Y. Kalachyova, V. Svorcik, O. Lyutakov, *Adv. Mater. Interfaces* **2017**, *4*, 1600886.

[23] X. Du, J. Li, A. Welle, L. Li, W. Feng, P. A. Levkin, *Adv. Mater.* **2015**, *27*, 4997.

[24] G. Godeau, T. Darmanin, F. Guittard, *J. Appl. Polym. Sci.* **2016**, *133*, 43130.

[25] Y. Sun, J. Ma, D. Tian, H. Li, *Chem. Commun.* **2016**, *52*, 4602.

[26] J. Osicka, M. Ilčiková, A. Popelka, J. Filip, T. Bertok, J. Tkac, P. Kasak, *Langmuir* **2016**, *32*, 5491.

[27] Y. Aono, A. Hirata, H. Tokura, *Appl. Surf. Sci.* **2016**, *371*, 530.

[28] T. D. Nelson, R. D. Crouch, *Synthesis* **1996**, *1996*, 1031.

[29] R. D. Crouch, *Synth. Commun.* **2013**, *43*, 2265.

[30] L. Pauling, *The Nature of the Chemical Bond and the Structure of Molecules and Crystals*, Cornell University Press, Ithaca, New York **1960**.

[31] A. A. Popova, S. M. Schillo, K. Demir, E. Ueda, A. Nesterov-Mueller, P. A. Levkin, *Adv. Mater.* **2015**, *27*, 5217.